A New Harmonic-based Protection structure for Meshed Microgrids

Siavash Beheshtaein[1], Rob Cuzner[2], Mehdi Savaghebi[1], and Josep M. Guerrero[1]

Aalborg University, Aalborg, Denmark[1]

University of Wisconsin Milwaukee, Milwaukee, USA[2]

{sib,mes,joz}@et.aau.dk, cuzner@uwm.edu

***Abstract*—This paper presents a novel harmonic-based overcurrent relay which detects and isolates three-phase faults in a meshed microgrid. The harmonic signals are generated by two Distributed Generators (DGs) which each of them communicate with its adjacent DG. In the first step, a set of features are extracted from DG output signal and then fed to a Support Vector Machine (SVM) to detect occurrence of fault. Once the fault is detected, based on minimum voltage measured by DG, two closest DGs will recognize and these two DGs inject two distinct harmonics to activate harmonic-based relays. As each set of relays located at either beginning or end of each section is activated by current with specific frequency, these relays behave like directional relays without using voltage transformers. As a result, the proposed method is cost-effective solution. The optimum Time Dial Settings (TDSs) of these relays are obtained by solving a coordination problem with Particle Swarm Optimization (PSO) algorithm. Real-time results are taken by OPAL-RT to show the effectiveness of the proposed method for two different locations of fault in a meshed microgrid.**

Index Terms*— Fault detection, isolation, harmonic injection, Relay coordination, support vector machine (SVM)

I. Introduction

Protection is considered to be one of the last barrier for realization of Microgrids (MGs). Microgrid protection faces several challenges including topology changes of microgrid and Distributed Generators (DGs) impacts that result in blinding of protection, sympathetic tripping, as well as weak-infeed loop fault [1]. On the other hand, meshed MG is a promising structure for the future MG to bring higher resiliency and reliability by adding redundant paths. Since in this structure, concept of upstream and downstream is not valid, the performance of conventional protective relays must be evaluated once again [2].

Fuses, reclosers, and overcurrent relays have no capability of isolate faults in looped microgrid with high penetration of DGs, and they require to be reset after any changes in the microgrid topology (i.e. islanding, isolation of sources, etc.) [3]. Distance relay has also low selectivity and cost of the voltage transformer needed for distance relays is high [4]. Similar to distance relays, directional relays utilize voltage and current transformers to determine the fault direction [5]. However, using directional relays is costly because both current and voltage transformers are needed. Although, differential relay addresses the problem of bidirectional power flow, the implementation cost of it is still high. Besides these conventional approaches, Fault Current Limiter (FCL) [6], and adaptive protection [7] have been presented to address the protection issues. The main disadvantages of these two approaches are high implementation cost and the need for a central monitoring unit, respectively.

This paper presents a novel directional protective relay that operates based on high-frequency harmonic current. Once the occurrence of fault is determined by using optimum selection of features, which are fed to a Support Vector Machine (SVM), the two nearest DGs inject two distinctive high-frequency signals. Each high-frequency signal activates a set of forward and backward relays. In order to achieve both fast response main and backup relays, Particle Swarm Optimization (PSO) algorithm is

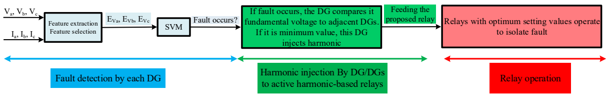

Fig. 1. Scheme of the proposed method.

used to find the optimum values of each directional relay parameters. Finally, different locations of fault are considered to validate the effectiveness of the proposed method.

II. Proposed Method

As shown in Fig.1, the proposed protection method consists of three main parts including fault detection, harmonic injection by DGs, and operation of high-frequency overcurrent relays with optimum settings. In the first step fault will be detected by feeding a proper set of features to the SVM classifier. Once the fault is recognize, the DG with minimum fundamental voltage, which means the DG that is closest to location of fault, injects high-frequency voltage/current. Finally, the high-frequency relays, which extract high-frequency component of current by Multiple Second-Order Generalized Integrators Phase Locked loop (MSOGI-PLL), will isolate the faulty line of the meshed microgid. It must be mentioned that these relays have been coordinated by optimum values of relays' settings.

A. Signal Processing Tools for Fault Detection

1) Feature Extraction and Feature Selection

In order to detect the fault, several features including standard deviation, RMS, energy, and Shannon-entropy are extracted from fundamental voltage/current signals. On the other hand, in order to increase the efficiency of SVM classifier in terms of complexity, computation time, and accuracy, the most relative and informative subset of features has to be selected. One of the widely used feature selection algorithms is the sequential forward selection method which starts with an empty feature set and adds a feature to the set until the accuracy does not change significantly [1]. In the present paper, this method is modified; the algorithm starts with the five best features and the conventional sequential forward selection method is applied to each of these features. The process continues until accuracy of fault classification reaches the desired value.

2) SVM

The SVM, which is a powerful binary classifier, adjusts a hyperplane to maximize the margin between two classes. This concept can be formulated as the following primal objective problem

$$\min j(\omega,\zeta) = \left\{\frac{1}{2}\|\omega\|^2 + C\sum_{i=1}^{n}\zeta_i\right\}$$

$$\text{S.t. } y_i(\omega^T\phi(x_i)+b) \ge 1-\zeta_i, \zeta_i \ge 0, y_i = \{-1,+1\}^n, \forall i = 1,2,\dots,n \quad (1)$$

where ζ, C, $\varphi(x_i)$ and y_i are the deviation from the margin, penalty factor, a function that maps the testing data vector x_i onto high-dimensional feature space, and the corresponding label for each x_i, respectively. Typically, the primal form of SVM (1) is solved by transforming it to a dual form utilizing Lagrange multiplier method.

$$\min L(\alpha) = \left\{\frac{1}{2}\sum_{i=1}^{n}\sum_{i=1}^{n} y_i y_j \alpha_i \alpha_j K(x_i,x_j) - \sum_{i=1}^{n}\alpha_i\right\}$$

$$\text{S.t. } \sum_{i=1}^{n}\alpha_i y_i = 0, 0 \le \alpha_i \le C \ \forall i = 1,2,\dots,n \quad (2)$$

where α_i, N, and $K(x_i,x_j) = \Phi(x_i)^T\Phi(x_i)$ are nonnegative Lagrangian multiplier, number of training data, and Kernel function, respectively. Among the different types of Kernel function, Gaussian Radial Basis Function (RBF) is selected in this paper that is defined as follows

$$K(x_i,x_j) = e^{-\gamma\|x_i-x_j\|^2} \quad (3)$$

where γ is the Kernel parameter.

The optimum decision function is achieved by solving this quadratic programming problem using training data with $\alpha_i^* > 0$ called support vectors [2]:

$$g(x) = sign(\textstyle\sum_{i\in SV}\alpha_i^* y_i . k(x,x_i) + b^*) \quad (4)$$

$$b^* = \frac{1}{N_{SV}}\left(\sum_{i=1}^{N_{SV}} y_i - \sum_{i=1}^{N_{SV}}\alpha_j^* y_i k(x_i,x_j)\right) \quad (5)$$

B. Harmonic injection

1) Harmonic Injection strategy

When a fault occurs in the meshed MG, two DGs are selected based on the lowest minimum measured fundamental voltage to inject two distinctive high-frequency harmonics. For example for a fault occurring in $Line_1$ (see Fig.2), first, DG_1 senses the lowest voltage and

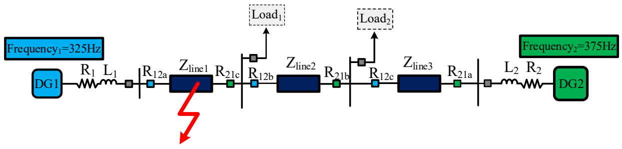

Fig. 2. An illustrative example demonstrating how the proposed harmonic-based relays works.

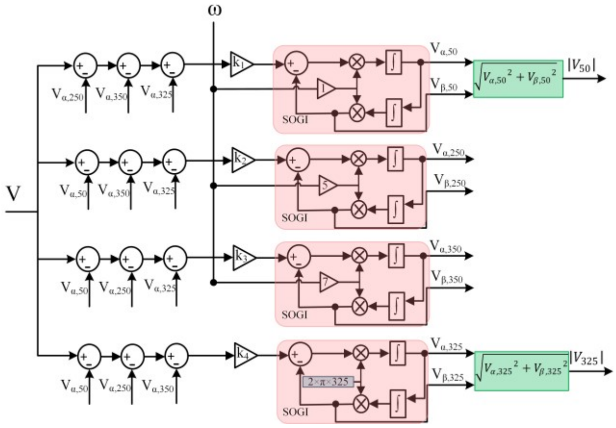

Fig. 3. MSOGI structure for fundamental and harmonic extraction of 325Hz.

injects harmonic signal of 325Hz. Due to this, current harmonic flows from DG_1 to the fault. In this case, the relays R_{12a}, R_{12b}, and R_{12c} measures harmonic current of 325 Hz, and among them, R_{12a} sends a tripping signal to its corresponding circuit breaker to make it open. Then, DG_2 senses the least minimum voltage and sends harmonic signal of 375 Hz to activate R_{21a}, R_{21b}, and R_{21c}. Finally, R_{21c} sends a tripping signal to open the corresponding circuit breaker. As it can be seen, regardless of microgrid topology and the number of DGs in microgrid, only one DG injects harmonic in each stage. This strategy makes microgrid system behave like a radial grid during the fault. Accordingly, one of the main challenges, which is bidirectional power flows, is addressed successfully.

2) Harmonic Selection and Detection

The selection of harmonic components frequency depends on different criteria, such as having no interaction with the LCL filter resonant frequency, grid resonant frequency, and fundamental frequency-dependent harmonics [3]. This paper chooses 325 Hz, 375 Hz, and 275 Hz as appropriate frequencies for the injected signal. In order to detect harmonic and fundamental components, MSOGI-based extraction is applied because of its good disturbance rejection capability; fast dynamic response and acceptable computational burden (see Fig. 3 for harmonic extraction of 325Hz).

3) Control System

Microgrids may operate in both islanded and grid-connected modes. In the grid-connected mode, voltage and frequency are maintained within the acceptable range by a stiff grid. However, in the absence of a stiff grid, at least one grid forming DG unit is required and other DGs could be grid following units. In this paper, one unit operates in Voltage Contolled Mode (VCM)/grid forming (Fig. 4) and others in Current Controlled Mode (CCM)/grid following (Fig. 4). As shown in Figs. 4 and 5, the current and voltage harmonic references of 325 Hz are added to the generated fundamental current and voltage references, respectively. Since DG has to inject a votage/current harmonics with 325 Hz independently in each phase, the topology of DG must be three-phase four-wire. Among different topologies of four-wire systems, the three-leg inverter with split dc-link capacitors is popular where the midpoint of the split dc-link capacitors is connected to a neutral point.

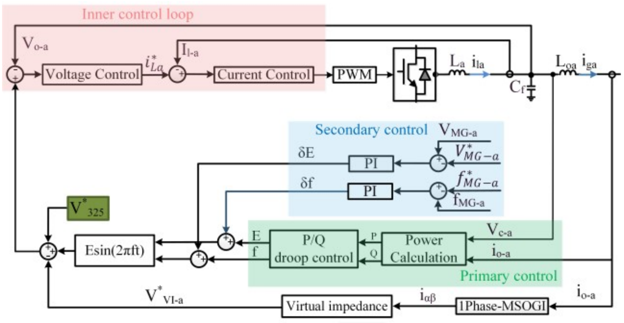

Fig. 4. Scheme of the voltage-control of phase-a of the three-phase four-wire DG with split dc capacitors.

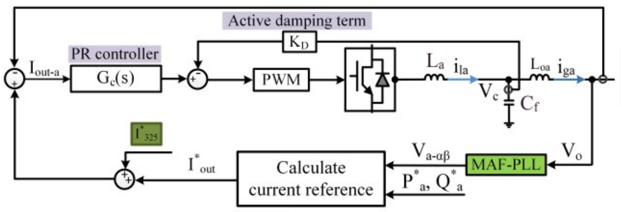

Fig. 5. Scheme of the current-control of phase-a of the three-phase four-wire DG with a split dc capacitors regarding harmonic injection.

As in natural (abc) reference frame Proportional Resonance (PR) controller has better performance than Proportional Integral (PI) one, in the inner loop control, PR controllers are considered for both VCM and CCM, as mentioned bellow:

$$G_V = k_V + \sum_{k=1,5,6,7} \frac{2.k_{rVk}.\omega_{cV}.s}{(s^2 + 2.\omega_{cV}s + (k\omega_0)^2)} \quad (6)$$

$$G_I = k_I + \sum_{k=1,5,6,7} \frac{2.k_{rIk}.\omega_{cI}.s}{(s^2 + 2.\omega_{cI}s + (k\omega_0)^2)} \quad (7)$$

where, ω_{cV} and ω_{cI} are the cut-off frequencies for current and voltage loops, respectively. In addition, $k_V(k_I)$ and $k_{rV}(k_{rI})$ are proportional and resonant coefficients of the voltage (current), respectively. In the secondary control level, PI controllers are applied to generate proper control signals to restore both frequency and voltage to their nominal values. As shown in Fig. 5, for CCM-inverter the current reference is generated according to active and reactive powers references. Then, similar to VCM-inverter, the current error passes through PR controller defined as follows [4]:

$$G_{CI} = k_{cI} + \sum_{k=1,5,6,7} \frac{2.k_{rIck}.\omega_{ccI}.s}{(s^2 + 2.\omega_{ccI}s + (k\omega_0)^2)} \quad (8)$$

C. Relay Coordination

1) Coordination formula

The purpose of each protection system is high-speed action of primary protection as well as well-coordination of backup relay with its primary one. This assumption could be formulated as follows:

$$Minimize: \sum_{i=1}^{N} t_i(x_{closed-in}) \quad (9)$$

$$subject\ to: TDS_{min} < TDS < TDS_{max}$$

$$t_{bj} - t_{mj} > CTI \quad \& \, t_{min} < t < t_{max}$$

where, t_i is operation time of primary relay for closed-in fault. The Coordination Time Interval (CTI) is minimum values between operation time of primary and backup relay. For numerical relay CTI as well as TDS_{min}, TDS_{max} and t_{min} is usually considered to be 0.1, 0.015, 1, 0.05. The operation time of the relay is typically considered to be as current-time characteristics, which is defined as follows:

$$t = \left(\frac{0.14}{\left(\frac{I_{fault}}{I_{pick}}\right)^{0.02} - 1} \right) .TDS \quad (10)$$

2) PSO algorithm

In order to find and optimum value of TDSs, PSO algorithm is used. This algorithm is formulated as follows:

$$V_i^{t+1} = \omega \times V_i^t + C_1 \times rand\,_1(.) \times (Pbest_i - X_i^t) + \cdots C_2 \times rand\,_2(.) \times (Gbest_i - X_i^t)$$

$$X_i^{t+1} = X_i^t + V_i^{t+1}$$

$$i = 1,2,3, \ldots, N \quad (11)$$

where C_1, C_2 are called learning factors and ω is inertia weight.

III. Real-Time Simulation Results

A meshed microgrid shown in Fig. 6 with its parameter (see Table I) is simulated in OPAL-RT with sampling time 20 ms to validate the effectiveness of the proposed method. In order to have highly efficient fault detection method, various conditions such as different load levels, load

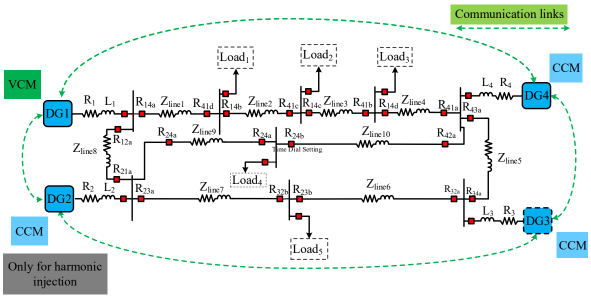

Fig. 6. System model.

switching, DG switching, line switching and transition from grid-connected mode to islanded mode as well as different amounts of fault resistance and fault locations are taken into account for training the SVMs (with C and γ parameters respectively equal to 4 and 10).Then, modified sequential forward selection algorithm is used to choose the best set of features. According to Table II, where inst. is short form of instantaneous, the selected features for fault detection include energy of phase voltages. As shown in Fig 6, only DG1, DG3, and DG4 provide active and reactive powers to the grid. However, DG2 is added to generate harmonic current for line6-line10 in forward direction (from left to right). It must be noted that each DG injects particular high-frequency harmonic signal for activating only forward/backward harmonic-based relays. For example in case of Line1,Line2, Line3, and Line4, DG1 and DG4 inject voltage harmonics of 325 Hz and 375Hz to forward relays (R14a, R14b, R14c, and R14d) and backward relays (R42a, R42b, R42c, and R42d), respectively. Due to this strategy, each set of forward/backward relays behaves like a directional relay without using voltage transformer. It must also be emphasized that optimum parameters of the relays are obtained by solving equations (9) and (10) by PSO algorithm. The resultant optimum values of IP and TDS of relays in Line1, Line2, Line3, and Line4 are presented in Table III.

In order to evaluate the effectiveness of the proposed method, two faults are exerted separately in different locations at 0.2s. First, a three-phase fault with Rf=0.4Ω is applied in Line 2 to examine the performance of proposed protection system. As shown in Fig.7 (a), the fault is detected in around 20 ms. Then, according to harmonic injection strategy, DG1 (Fig. 7 (e)), injects voltage harmonic of 33 volt at 325 Hz to activate forward relays. After around a 0.4 s, the tripping signal is sent to proper forward relay, which is R14b, (Fig.7 (f)) to disconnect one side of faulted line.

While R14b disconnects one side of the faulty line, DG4 will be closest DG to the fault and subsequently experiences the minimum fundamental voltage. Then this DG injects a 2A current at 375 Hz Fig.7 (g)). This harmonic current activates R41C, at 0.8s (Fig.7 (h)). As it can be seen in Figs. 7(b),(c),(d), the proposed protection system effectively detects and isolates the fault in less than 0.6 s. Similarly, a three-phase fault with Rf=0.1Ω have been placed in Line10 at 0.2s. As represented in Fig. 8, once the fault is detected, DG4 injects harmonic current of 2A at 375 Hz to activate backward relays. Then, R42a operates at 0.35s (Fig.8 (g)). After that, DG2 injects harmonic of 2A at 275 Hz to let the forward relays work. As shown in Fig. 8(f), R24b sends a tripping signal at 0.45s. These two results clearly show that the proposed protection system has the capability to detect and isolate fault in the least possible time.

TABLE I. System parameters

Type	Parameters		Value
	Symbol	Quantity	
Electrical setup	V_{dc}	DC Voltage	650 V
	V_{MG}	MG voltage	311 V
	F	MG Frequency	50 Hz
	C	Filter Capacitance	25 µF
	L	Filter Inductance	1.8 mH
	L_o	Output Inductance	1.8 mH
	P_{L1}	Constant active power load	1500 W
	P_{L3}, P_{L4}	Constant active power load	1000 W
	R_{L2}, R_{L5}	Constant resistive load	70.53 Ω
	Z_{line1} to Z_{line10},	Line resistance	1+j0.43 Ω
	Z_{L2}, Z_{L9}	Line resistance	2+j0.86 Ω
Primary control	k_{pV}	Proportional coefficients of voltage	1
	k_{rV}	Resonant coefficients of voltage	50
	k_{pI}	Proportional coefficients of current	20
	k_{rI}	Resonant coefficients of current	1000
	ω_{cV}	cut-off frequency of voltage loop	2 Hz
	ω_{cI}	cut-off frequency of control loop	2 Hz
	k_{pII}	Proportional coefficients of current	300
	k_{rII}	Resonant coefficients of current	2500
	ω_{cII}	cut-off frequency of control loop	2 Hz
	k_D	Damping factor	300
	R_{v50}	Virtual for 50 Hz	4 Ω
	R_{v275}	Virtual resistance for 275 Hz	44 Ω
	R_{v325}	Virtual resistance for 325 Hz	44 Ω
Droop Control	k_{pP}	Active power droop term	0.0003 Ws/rad
	k_{iP}	Active power droop integral term	0.0015 Ws/rad
	k_{pQ}	Reactive power droop term	0.2 VAr/V
Secondary Control	k_{pf}	Frequency proportional term	0.01
	k_{if}	Frequency integral term	1 s^{-1}
	k_{pE}	Voltage proportional term	0.1
	k_{iE}	Voltage integral term	10 s^{-1}

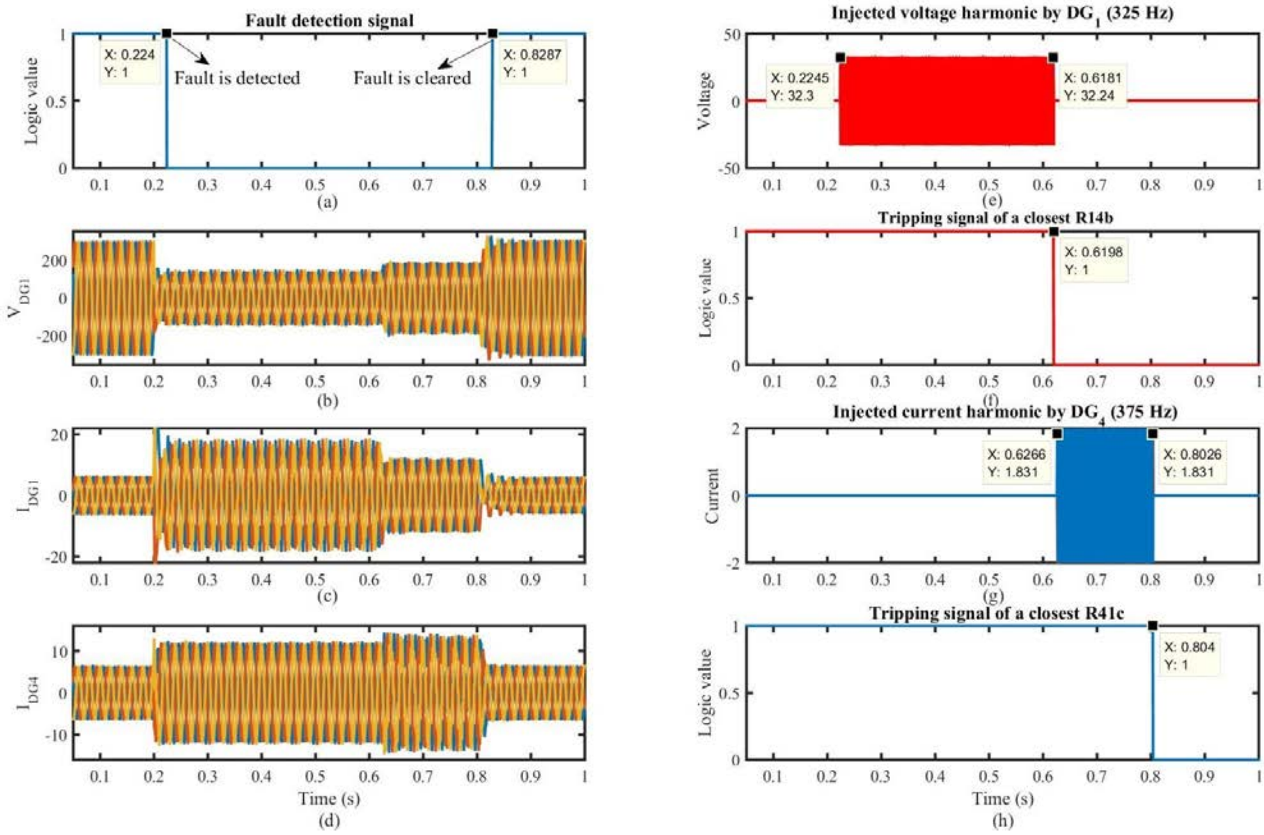

Fig. 7. Realtime simulation results for fault applied on $Line_2$.

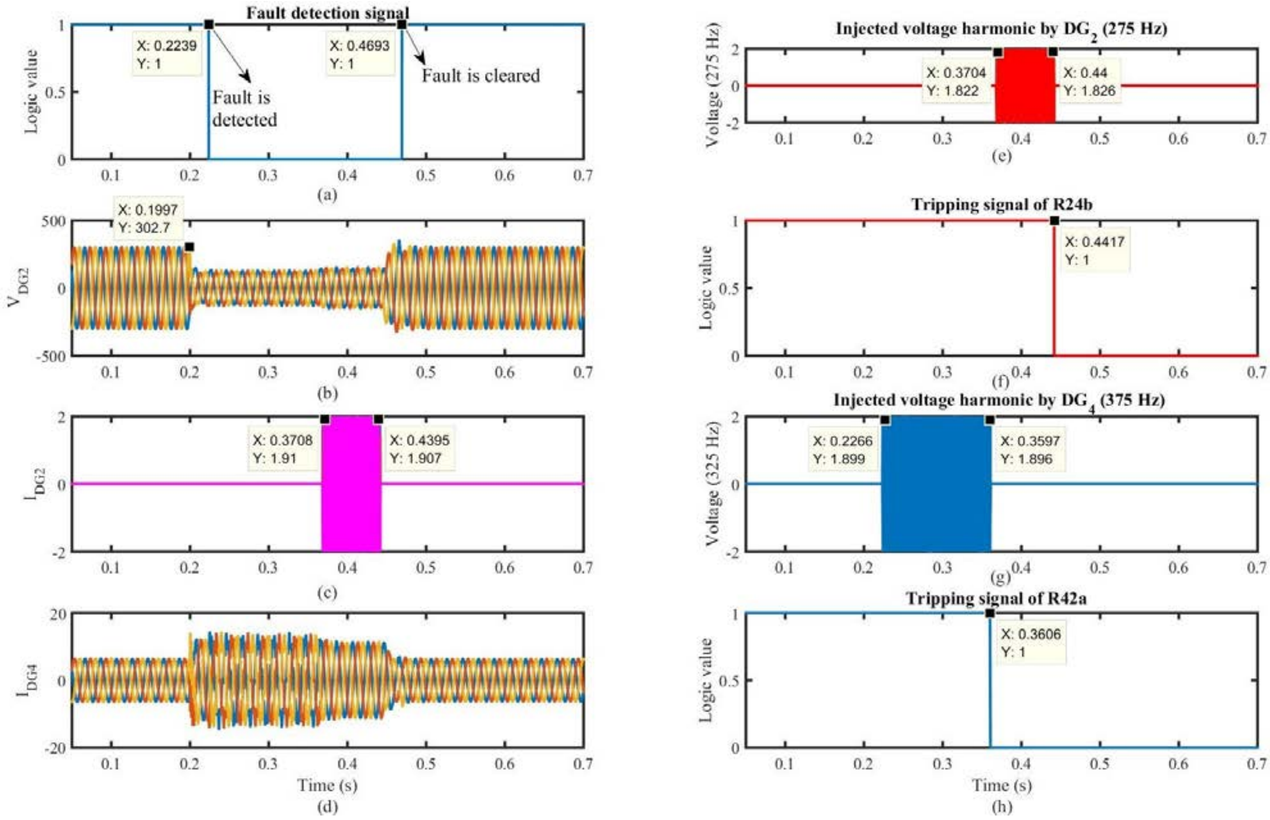

Fig. 8. Realtime simulation results for fault applied on $Line_{10}$.

TABLE II. Feature selection for fault detection based on modified sequential forward algorithm.

Selected Features in each step	**Class Type Accuracy**	
	Normal	**ABCG**
Energy (I_C)	70 %	55 %
RMS (I_C)	50 %	100 %
Energy (V_C)	0 %	83.33 %
RMS (V_C)	0 %	94.44 %
Inst.(V_c)	0 %	94.44 %
Energy (I_C) & Energy(V_A)	100 %	94.44 %
RMS (I_C) & RMS (V_B)	50 %	94.44 %
Energy(V_C) & Energy(V_B)	50 %	100 %
RMS (V_C) & Inst.(V_B)	0 %	94.44 %
Inst.(V_c) & Inst. (V_B)	40 %	88.89 %
Energy(I_C) & Energy(V_A)& Energy(V_B)	100 %	100 %
RMS (I_C) & RMS (V_B) & Inst. (V_A)	80 %	94.44 %
Energy(V_C)&Energy(V_B)& Energy(V_A)	**100 %**	**100 %**
RMS (V_C) & Inst. (V_B) & Inst. (V_A)	100 %	94.44 %
Inst. (V_c) & Inst. (V_B) & Inst. (I_A)	60 %	88.89 %

TABLE III. Optimum valuse of TDSs and pickup currents for the relays in $Line_1$, $Line_2$, $Line_3$, and $Line_4$.

Relay number	I_p	**TDS**
R_{14a}	3 amp (325 Hz)	0.0175
R_{14b}	2.5 amp (325 Hz)	0.0183
R_{14c}	2.45 amp (325 Hz)	0.0154
R_{14d}	2.35 amp (325 Hz)	0.0069
R_{41a}	1 amp (375 Hz)	0.0190
R_{41b}	0.8 amp (375 Hz)	0.0183
R_{41c}	0.6 amp (375 Hz)	0.0175
R_{41d}	0.5 amp (375 Hz)	0.0069

IV. CONCLUSION AND FUTURE WORKS

In this paper, a new high-frequency protection relays is proposed to detect and isolate fault by injecting harmonic signals. According to the strategy of harmonic injection, only one DG takes the responsibility of activation of the corresponding relays. As a result, the relays behave like directional relays. The main advantage of this method is that the resultant directional relays do not need any voltage transformer to detect direction of fault. Therefore, it is a cost-effective solution for microgrid protection.

The real-time simulation results show that the fault is detected in around 20ms. In this process, two DGs sequentially inject distinctive harmonic signal to activate their corresponding relay. Regarding the optimum values of the protection relays, the fault is isolated after around 0.5s.

The results of two simulation scenarios are shown to validate the effectiveness of the proposed method. In final version, more results for other types of faults (i.e AB and AG faults) will be presented.

REFERENCES

[1] Huseyin Eristi, A. Ucar, and Y. Demir, "Wavelet-based feature extraction and selection for classification of power system disturbances using support vector machines," *Electr. Power Syst. Res.*, vol. 80, pp. 743–752, 2010.

[2] H. Livani, S. Member, C. Y. Evrenosoglu, and S. Member, "A Machine Learning and Wavelet-Based Fault Location Method for Hybrid Transmission Lines," *IEEE Trans. Smart Grid*, vol. 5, no. 1, pp. 51–59, 2014.

[3] D. D. Reigosa, F. Briz, S. Member, C. B. Charro, P. García, and J. M. Guerrero, "Active Islanding Detection Using High-Frequency Signal Injection," *IEEE Trans. Ind. Appl.*, vol. 48, no. 5, pp. 1588–1597, 2012.

[4] J. He and Y. W. Li, "Generalized Closed-Loop Control Schemes with Embedded Virtual Impedances for Voltage Source Converters with LC or LCL Filters," *IEEE Trans. Power Electron.*, vol. 27, no. 4, pp. 1850–1861, 2012.

[5] L. Chen, H. Chen, Z. Shu, G. Zhang, T. Xia, and L. Ren, "Comparison of Inductive and Resistive SFCL to Robustness Improvement of a VSC-HVDC System With Wind Plants Against DC Fault," *IEEE Trans. Appl. Supercond.*, vol. 26, no. 7, 2016.